# Isothermal dynamics simulations of spontaneous alloying in a microcluster

Taizo R. Kobayashi* and Kensuke S. Ikeda†
*Department of Physics, Faculty of Science and Engineering, Ritsumeikan University, Noji-higashi 1-1-1, Kusatsu 525-8577, Japan*

Yasushi Shimizu
*Fukui Institute for Fundamental Chemistry, Kyoto University, Takano-Nishihiraki-cho 34-4, Sakyou-ku, Kyoto 606-8103, Japan*

Shin-ichi Sawada
*School of Science and Technology, Department of Physics, Kwansei Gakuin University, 2-1, Gakuen, Sanda 669-1337, Japan*
(Received 16 October 2002; revised manuscript received 12 July 2002; published 17 December 2002)

Dynamics of surface atoms penetrating into microclusters is investigated in connection with the very rapid alloying phenomenon in metal microclusters first discovered by Yasuda, Mori M. Komatsu, K. Takeda, and H. Fujita, J. Electron Microsc. **41**, 267 (1992). A new algorithm to simulate the cluster dynamics where isothermal condition is satisfied without adding any stochastic noise is developed in order to suppress gradual temperature rise due to the emission of reaction heat. The dependence of radial diffusion and alloying processes on temperature and negative heat of solution are elucidated separately. The diffusion process obeys an Arrhenius-like law, and unexpectedly, the radial diffusion rate is not very sensitive to the magnitude of negative heat of solution. This fact implies that the rapid diffusion is not a peculiar feature of binary clusters but a universal feature of small clusters. However, the magnitude of negative heat of solution still dominates the alloying process through a preexponential factor. The mechanism causing the rapid radial diffusion is quite different from the mechanism of diffusion in bulk solid, and very active motion of atoms along the surface of cluster plays a crucial role. Based upon our quantitative results, the mechanism with which the surface activity is converted into the rapid radial diffusion is discussed.

DOI: 10.1103/PhysRevB.66.245412 PACS number(s): 61.46.+w, 66.30.Jt, 67.80.Mg, 02.70.Ns

## I. INTRODUCTION

Nanosized microclusters consisting of less than $10^3 - 10^4$ atoms have very curious features which cannot be observed in bulk systems. A number of interesting static and dynamical properties of nanosized clusters have been reported by many authors during last two decades.[2] A remarkable feature of microcluster is its dynamical activity. Rapid shape transformation of small Au clusters on a substrate, which was first observed by Iijima,[3] is a typical example manifesting the dynamical activity of microclusters. Such a phenomenon allows for some kinematical interpretations based upon the shallow multibasin structure of free-energy function.[4,5] Sawada and Sugano showed that the rapid shape transformation may be spontaneously induced by the *deterministic* chaotic dynamics of the cluster itself without any thermal agitation from the external environment.[6–8] Wandering motion of clusters among various shapes is very similar to a chaotic itinerancy among destabilized attractors.[9–11] Another example of the dynamical activity of microcluster is the ''coexisting phase'' between solid and liquid, which was first reported by Berry and his co-workers on the basis of their deterministic dynamical (i.e., microcanonical) simulations of a Lennard-Jones cluster.[12] In many aspects, the dynamical activity of microclusters seems to be attributed to a very large fluctuation due to the deterministic chaotic motion. A remarkable feature peculiar to the microcluster is that considerable part of the constituent atoms are on the surface along which atoms can move very actively, in other words, the surface of cluster melts[13,14] Such a feature seems to be an essential origin of dynamical activity in microclusters.

In 1992 Yasuda and Mori(YM) discovered a very interesting phenomenon manifesting the dynamical activity of microclusters by using transmission electron microscope. They observed that the solute atoms (e.g. Cu atom) deposited on the surface of nanosized metal cluster (e.g. Au cluster) on a substrate are promptly absorbed into the host cluster. A highly concentrated and homogeneously mixed alloyed cluster is formed at room temperature.[1] Figure 1 illustrates their *in situ* observation. Such a rapid alloying process is often called *spontaneous alloying* (SA). YM explored extensively the presence of SA for a variety of combinations of solute atom (hereafter referred to as *guest* atom) and the host cluster such as (Au,Ni),(In,Sb),(Au,Zn), and (Au,Al), and they confirmed that SA is a universal phenomenon in nanosized binary metal clusters. Their experimental results can be summarized in the following items:

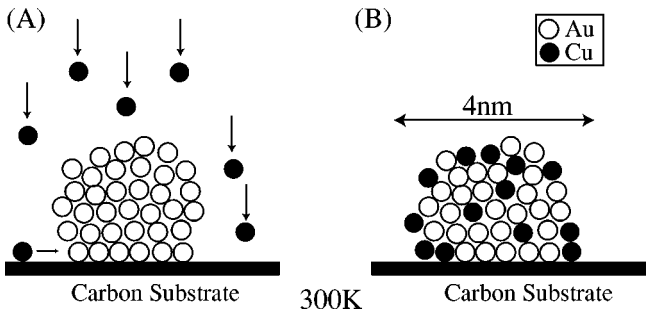


FIG. 1. Schematic illustrations of *in situ* observation of the SA by YM. (A) individual copper atoms are deposited on a gold cluster. (B) SA is completed. Copper atoms dissolve into a gold cluster to form a homogeneously mixed alloy cluster.

 

(1) In case of Cu-Au cluster the estimated diffusion rate is more than $10^9$ times faster than that in the bulk medium.

(2) Complete alloying is observed in the cluster less than a critical size. For clusters larger than the critical size, the alloying takes place only in a shell-shaped region beneath the free surface of individual cluster and a core composed only by the host metals is retained.

(3) The critical radius increases with the modulus of negative heat of solution. For the combination of species with sufficiently large positive heat of solution, SA does not occur.

(4) The SA occurs in the solid phase of the cluster.

Quite recently, Kimura, Kaito, and their co-workers observed that alkali halide microclusters composed of (KCl, KBr) and some other combination of ionic species also form a mixed cluster within sec at room temperature.[15] These observations strongly imply that the very rapid formation of mixed cluster is not a peculiar feature of metal clusters but a universal feature of general kind of binary microclusters.

To understand the dynamics of SA, Shimizu, Sawada, and Ikeda (SSI) examined numerical simulations by using two-dimensional (2D) Morse cluster.[16,17] Since their final purpose is to elucidate the role of deterministic chaos in SA, they used a microcanonical simulation based on the Newton's equation of motion. They demonstrated that the SA occurs in the solid phase if the heat of solutions is negative. Further, they elucidated a remarkable size effect and temperature dependence of the alloying process. Thus the essential features of YM's experiments summarized in the above items were well reproduced in their simulation. However, to understand the actual process of SA and its underlying mechanism, there still remain several basic problems to be overcome. SSI used the microcanonical simulation, which means that the system is isolated and total energy is conserved. As a result, because of the emission of reaction heat in the progress of alloying, the heating up of the cluster makes their results ambiguous and confusing: in order to make the time required to complete alloying (say, the alloying time) shorter than a microsecond, which is the upper bound accessible by recent computational ability, their simulation was done in a relatively high-temperature regime of the solid phase. Under the isoenergetic condition the emitted heat pushes the temperature up toward the melting temperature and hence influences considerably the SA process. As was shown by SSI, the alloying time crudely exhibits an Arrhenius-like temperature dependence, and hence it is very sensitive to the temperature rise. Therefore, it was impossible to establish how the SA depends separately on the key parameters such as temperature, negative heat of solution, and cluster size, and so on.

A more practical requirement comes from the experimental situation. The experiment of SA is observed in the clusters placed on the substrate of amorphous carbon film. The emitted heat may be released to the substrate on the time scale much shorter than the alloying. In fact YM obtained a strong experimental evidence that there is no significant temperature rise in the alloying process.[18,19] Since the experiment is done under the constant temperature condition, it is necessary to take account of the effect introduced by the isothermal condition. Based on the above considerations, it is strongly desired to reexamine the simulation of SA under an isothermal condition and compare its results with that under an microcanonical condition. This is just the purpose of the present paper.

For the purpose of technological applications there have been a number of researches for the diffusion process of atoms in the bulk media.[20] However, quite few deal with the diffusive penetration of atoms into microclusters, probably because of experimental difficulties. What we would like to make clear is the mechanism of very rapid diffusion into the microclusters, which will not be peculiar to binary clusters but universal in microclusters. For this purpose, first of all we should explore the *activation process* behind the diffusion process, which is also fundamental in the conventional investigations of atomistic diffusion in bulk media.[20] Such a research is possible only under the temperature controlled condition. In the present paper we investigate the detailed features of SA for a model 2D cluster under the temperature controlled condition. In particular, we concentrate ourselves to elucidating the effect of heat of solution and the effect of temperature, which cannot be resolved separately in the microcanonical simulation. The size effect will be reported in a subsequent paper.

The present paper is organized as follows. In Sec. II we propose a temperature controlling algorithm suitable for our purpose. We discuss in detail why the proposed algorithm is adequate for the isothermal simulation of SA. The model Hamiltonian and the initial configurations of our simulation together with standard tools used in the data analysis are introduced and discussed. Sec. III is the main part of the present paper. First of all, in Sec. III A we demonstrate that the size of cluster is a crucial factor of SA. Fixing the size of cluster to a typical one, we focus our attention to the dependence of SA on temperature and negative heat of solution. In Sec. III B we investigate the activation process of diffusive motion in radial direction of cluster. By the method of optimal Arrhenius scaling, the activation energies associated with the radial motion of atoms are evaluated as precisely as possible, and some unexpected features of the diffusion process and the alloying process (these two should conceptually be distinguished) are elucidated for the first time by the isothermal simulation. Finally in Sec. III C we discuss the relation between the radial diffusive motion and the very rapid diffusion along the surface of cluster. A direct evidence that the surface diffusion controls the SA is presented in Sec. III D, and the mechanism with which the surface motion is converted into the radial diffusion is discussed in Sec. IV, which is devoted to the conclusion and discussion of the present paper.

## II. PROCEDURE OF SIMULATION

In this section we discuss the algorithm used in our simulation together with the model potential and the initial conditions.

### A. Averaged kinetic-temperature controlling method

Several algorithms, such as instantaneous velocity scaling method, Nose's method etc, with which the kinetic temperature is controlled accurately to a desired level have been proposed.[21–25] These methods are very powerful for the isothermal simulation of bulk systems done under the periodic

boundary condition. Unfortunately, these methods cannot be directly applied to cluster systems with free surface, in particular, to the alloying clusters which are far from the equilibrium and emit considerable amount of heat in the simulation process. Indeed, we examined these methods by microclusters, and we often observed some undesired phenomena such as uncontrollable evaporation of surface atoms and dissociation of the cluster.[26]

We recall that we want to control is not the kinetic temperature defined at every instance, but the averaged kinetic temperature that increases very slowly on a very long time scale of alloying. The method we introduce here suits our aim, namely, it controls the kinetic temperature averaged over such a long time interval that it is well defined.

For sake of simplicity we consider a two-dimensional (2D) cluster which has no total momentum and no total angular momentum. The instantaneous kinetic temperature is then defined by $T(t)=[2E_k(t)/(2N-3)k_B]$, where $E_K(t)=\Sigma_{i=1}^{N}\mathbf{p}_i^2/2m$ is the total kinetic energy of the cluster at the time $t$ and $N$ is the number of constituent atoms. Let $\hat{T}(t)$ be the averaged kinetic temperature defined over the time interval of $\tau$ preceding $t$,

$$\hat{T}(t)=\int_{t-\tau}^{t}T(t')dt'/\tau. \tag{1}$$

By ''temperature'' we hereafter mean such a time-averaged kinetic temperature over a sufficiently long time scale $\tau$ containing more than a few hundreds of Debye oscillations. Let $T$ be the target temperature to be realized, then we rescale the momentum $\mathbf{p}_i$ of each constituent atom $i$ according to

$$\mathbf{p}_i'(t)=\sqrt{\frac{\hat{T}(t)-\varepsilon(\hat{T}(t)-T)}{\hat{T}(t)}}\mathbf{p}_i(t), \tag{2}$$

where $\varepsilon$ is a positive parameter much less than the unity. Such a procedure is repeated at every $\tau$, ie. at $t=n\tau$ ($n$ = integer), and in the interval $n\tau<t<(n+1)\tau$ between the successive two scaling processes, the trajectory is propagated by the Hamilton's equation of motion.

$$\dot{\mathbf{q}}_i(t)=\frac{\partial H(\{\mathbf{q}_i\},\{\mathbf{p}_i\})}{\partial\mathbf{p}_i},$$

$$\dot{\mathbf{p}}_i(t)=-\frac{\partial H(\{\mathbf{q}_i\},\{\mathbf{p}_i\})}{\partial\mathbf{q}_i}.$$

We denoted the total energy, which is conserved in the interval $n\tau<t<(n+1)\tau$, by $E_n$. Let the total potential energy be $U(t)$ and define $V(t)=2U(t)/[k_B(2N-3)]$, then by using the identities $2E_n/[k_B(2N-3)]=\hat{T}(n\tau)+\hat{V}(t)(n\tau)$ and $2(E_{n+1}-E_n)/[k_B(2N-3)]=T(n\tau+0)-T(n\tau-0)$ together with Eq. (2), it immediately follows that

$$\frac{\hat{T}((n+1)\tau)-\hat{T}(n\tau)}{\tau}=-\frac{\varepsilon_n}{\tau}[\hat{T}(n\tau)-T]+J((n+1)\tau), \tag{3}$$

where $\varepsilon_n\equiv\varepsilon T(n\tau-0)/\hat{T}(n\tau)(>0)$, and $J((n+1)\tau)\equiv-\hat{V}((n+1)\tau+\hat{V}(n\tau))/\tau$. Since the time-averaged quantity such as $\hat{T}_n=\hat{T}(n\tau)$ and $\hat{V}_n=\hat{V}(n\tau)$ do no longer fluctuate violently and they can be looked upon as slowly varying functions of the discrete time $t=n\tau$. Therefore, $\hat{T}((n+1)\tau)-\hat{T}(n\tau)/\tau$ etc. can be replaced by the derivative $d\hat{T}(t)/dt$, and Eq. (3) is approximated by a differential equation

$$d\hat{T}(t)/dt=-\gamma(t)[\hat{T}(t)-T]+J(t), \tag{4}$$

where $J(n\tau)=(\hat{V}(n\tau)-\hat{V}((n+1)\tau))/\tau\sim-d\hat{V}(t)/dt$ is the source term which almost takes positive values in case of the alloying problem because the total potential energy decreases through the alloying process.[16,17] Equation (4) can be interpreted as a relaxation equation for the time-averaged kinetic temperature $\hat{T}$, and the relaxation term multiplied by the effective relaxation rate $\gamma(n\tau)\equiv\varepsilon_n/\tau$ suppresses the deviation of the averaged kinetic temperature from the target temperature $T$ against the heating up due to the source term $J(t)$. Note that the instantaneous temperature $T(n\tau-0)$ is the sum of the kinetic energy of $N$ particles, and so its relative fluctuation around the averaged quantity $\hat{T}(n\tau)$ is at most $O[1/\sqrt{N}]$ if dynamics governed by the Hamilton's equation of motion is fully chaotic. We may thus approximate $\varepsilon_n\sim\varepsilon$ and $\gamma(t)\sim\gamma\equiv\varepsilon/\tau$, and Eq. (4) yields

$$\hat{T}(t)-T=\int_0^t e^{-\gamma(t-s)}J(s)ds \tag{5}$$

Now we suppose that the magnitude of the source term is bounded from above such that $|J(t)|<J$, then

$$\frac{|\hat{T}(t)-T|}{T}<\frac{J}{T\gamma}. \tag{6}$$

Let $\Delta U$ be the decrement of the total potential energy when the alloying is achieved at the *alloying time* $t_{alloy}$, then $J\sim2\Delta U/[(2N-3)k_Bt_{alloy}]$, and the sufficient condition for keeping the averaged kinetic temperature close to the given target $T$ is

$$\gamma=\frac{\varepsilon}{\tau}\gg\frac{2\Delta U}{(2N-3)k_BTt_{alloy}}. \tag{7}$$

The $\Delta U$ will be estimated in Sec. II D. In typical alloying process, the right-hand side is so small that we may choose $\varepsilon$ small enough (typically less than 0.01) and $\tau$ sufficiently long (typically more than 10 ps). With these values we achieved a kinetic temperature control less than a few percent.

The system behaves as an isolated system obeying the deterministic Hamilton's equation of motion except at the instants of the rescaling. Moreover, the effect of the rescaling procedure on the trajectory is extremely small. The present algorithm meets our requirement that the average kinetic temperature is controlled to a desired level keeping the modifications to the original law of motion as small as possible.

Our model does not, of course, generate canonical ensemble in a mathematically rigorous sense, but it is confirmed that subsystems obey canonical distribution at the

temperature $T$. In particular, the velocity distribution of any sampled atom in the cluster exhibits Maxwell-Boltzmann distribution. Detailed stability analyses for a generalized form of our scheme will be presented in a forthcoming paper, in which comparison with the well-known Langevin algorithm will be also done.[26]

### B. Model

The potential part of our model Hamiltonian

$$H=\sum_{i=1}^{N}\frac{1}{2m}\mathbf{p}_i^2+\sum_{i<j}V_{kl}(|\mathbf{q}_i-\mathbf{q}_j|) \tag{8}$$

is the Morse potential that was used in the previous paper,[17]

$$V_{kl}(r)=\epsilon_{kl}\{e^{-2\beta_{kl}(r-\sigma_{kl})}-2e^{-\beta_{kl}(r-\sigma_{kl})}\}, \tag{9}$$

where the suffixes $k$ and $l$ specify the two species of atoms, say *host* and *guest* atoms. Host and guest atoms are denoted by $A$ and $B$, respectively. A cluster contains $N_A$ host atoms and $N_B$ guest atoms, and the total number of atoms is $N=N_A+N_B$. We choose $\beta_{AA}=\beta_{BB}=\beta_{AB}=1.3588[A^{-1}]$, $\epsilon_{AA}=\epsilon_{BB}=\epsilon=0.3429\ [eV]$ and $\sigma_{AA}=\sigma_{BB}=\sigma_{AB}=2.866[A]$, which correspond to the values for Cu atoms.[27] Finally, the only free parameter

$$\alpha=\epsilon_{AB}/\epsilon_{AA} \tag{10}$$

controls the heat of solution in the binary system. It is a key parameter of the SA process. In fact, the heat of solution $\Delta H$ in the bulk medium given by

$$\Delta H=z(1-\alpha)\epsilon, \tag{11}$$

where $z$ is coordination number. The choice $\alpha>1$ and $\alpha<1$ indicates the negative and positive heat of solution, respectively.

The reasons why we use such a simple kind of two-body potential instead of more realistic many-body potential devised for the simulation of metals were fully discussed in Ref. 17, and we do not repeat it here. Results of simulation based upon many-body potential will be discussed in Ref. 28.

Our simulation is performed in the two dimension. The main reason why we use the 2D cluster is that the computation time for the 2D model is much shorter than the 3D model. Since the alloying is a very slow process, the computation time required for an alloying process to complete exceeds microsecond. A 4 nm-sized 3D cluster exhibiting the SA contains more than a few thousand atoms, and a simulation for such a cluster over microsecond is beyond the present computational capability. Based on the results of our preceding works,[16,17] we become strongly confident that our 2D simulation reproduces the essence of experimentally observed features summarized by the four items in the Introduction.

We integrated the Hamilton's equations of motion by the velocity-Verlet algorithm with the step-size $10^{-2}$ ps. The velocity rescaling procedure is done at every $\tau>10$ ps and $\epsilon=0.01$.

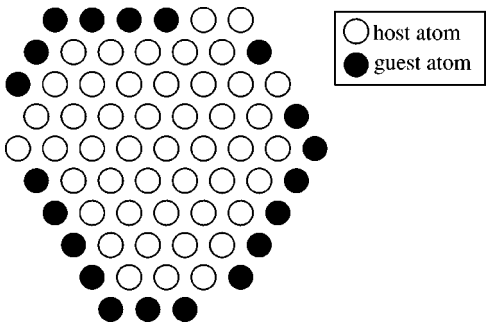


FIG. 2. A typical initial atomic configuration for MD simulation. White and black circles denote host($A$) and guest($B$) atoms. This cluster consists of 47 host and 20 guest atoms.

### C. Initial configuration

The initial configuration of the binary cluster from which the simulation starts is prepared in a similar procedure as in Ref. 17. First, we suppose that the cluster is composed of a single species of atom, and make it relax to the equilibrium state at a given temperature $T$ by applying the average velocity scaling algorithm. Next, we replace most of atoms on the surface of cluster with guest atoms. We regard it as the initial configuration and continue simulation by the procedure described in Sec. II A. In the present paper various size of clusters of total atom number $N=67$, 117, and 200 are examined. Among them we extensively test the $N=67$ clusters composed of $\sim 6$ layers. A typical example of the initial configuration of the $A_{47}B_{20}$ is depicted in Fig. 2.

As we are interested in the alloying of process of the clusters in the solid phase, the simulation is done well below the melting temperature $T_M$, which is decided by the caloric curve. It is obtained by successive microcanonical simulations changing the total energy at a small grid. We identify the time-averaged kinetic temperature at which a discontinuous jump occurs in the caloric curve as the melting temperature $T_M$.[13] As the cluster is finite sized, it is in principle impossible to locate the rigorous $T_M$: the ''melting'' state is distinguishable from the ''nonmelting'' state only within a finite time scale. Indeed, $T_M$ fluctuates considerably depending upon the size of the cluster and the time over which the averaged kinetic temperature is defined. We, however, decide the melting temperature $T_M=750\pm 50$ K for the cluster of the standard size ($N=67$) mainly examined in the present paper.

### D. quantities characterizing alloying dynamics

First of all we define the mean distance of the guest atoms $R(t)$ measured from the center of mass of the cluster, which is fixed and is chosen as the origin because the total momentum vanishes,

$$R(t)=\frac{1}{N_B}\sum_{i\in\text{guest atoms}}|\overline{\mathbf{q}_i}(t)|. \tag{12}$$

To eliminate very rapid vibrations of atoms around the equilibrium positions (typical period is the inverse of the Debye

frequency $\omega_D^{-1} \sim 0.1$ ps), we take the smoothed data $\overline{\mathbf{q}}(t) \equiv \int_{t-\Delta t}^{t} \mathbf{q}(t')dt'/\Delta t$ averaged over a time interval $\Delta t \sim 10$ ps $\gg \omega_D^{-1}$ around $t$. Since the guest atoms are initially on the surface, $R(t)$ decreases as the alloying proceeds, and $R(t)$ measures how the guest atoms diffuses into the cluster, but it does not provide information about relative arrangement of the two atomic species, which is the most important feature of the alloying process. We introduce a quantity directly measuring such a feature.

If the heat of solution of the binary system is negative, the $B$ atoms energetically prefer to be encircled by the host atoms. We define the number of neighboring host atoms per a guest atom as

$$n_B(t) = \frac{1}{N_B} \sum_{i \in \text{guest atoms}} N_{A(i)}(t), \tag{13}$$

where $N_{A(i)}(t)$ is the number of the nearest-neighbor host atoms around the $i$th $B$ atom at time $t$. This is a simple but useful measure of the alloying process.[16] If the interaction between the two atoms more distant than the nearest-neighbor distance is neglected, the temporal change of total potential energy $\Delta U$ from the initial value is related to $\Delta n_B(t) = n_B(t) - n_B(t=0)$, i.e., the deviation of $n_B$,

$$\Delta U = -\epsilon(\alpha - 1) N_B \Delta n_B . \tag{14}$$

Thus $n_B(t)$ is roughly proportional to the energy gain due to the formation of the alloyed state. If the two species of atoms are uniformly mixed, $n_B(t)$ should be $n_B^c = z(1-r)$, where $r = N_B/(N_A + N_B)$. $n_B(t)$ generally increases starting from $n_B(t=0)$, which is decided by the initial configuration and approaches the value $n_B^c$ as the alloying proceeds. $n_B(t=0)$ in Fig. 2 is $\sim 2.1$, while $n_B^c$ is $\sim 4.2$ for the $A_{47}B_{20}$ cluster.

The third quantity measures the activity of rearrangement of atoms, namely, the frequency of recombination of the neighboring atoms, which is estimated by the distance index.[7] Distance index is derived from a adjacency matrix $A(t)$, which is the $N \times N$ symmetric matrix whose elements are

$$A_{ij}(t) = \begin{cases} 1: & \overline{r}(t)_{ij} \leqslant \sqrt{2}\sigma \\ 0: & \overline{r}(t)_{ij} > \sqrt{2}\sigma \end{cases}, \tag{15}$$

$\overline{r}(t)_{ij} = |\overline{\mathbf{q}}_i(t) - \overline{\mathbf{q}}_j(t)|$ is the average distance between $i$ and $j$ atoms. The distance index $d_i(t)$ of the $i$th atom is, then defined by

$$d_i(t) = \sqrt{\sum_j |A_{ij}(t+\Delta t) - A_{ij}(t)|^2}. \tag{16}$$

This measures the number of the recombining events around the $i$th atom and characterizes the mobility or the activity of the individual atom, where $\Delta t$ is taken short enough to catch each recombination event which occurs at the frequency $\sim 10$–$100$ ps. We usually set $\Delta t \sim 10$ ps. The accumulated distance index per an atom, which is defined by

$$S(t) = \sum_{n=1}^{t/\Delta t} \left\{ \sum_{i=1}^{N} \frac{d_i(n\Delta t)}{N} \right\}, \tag{17}$$

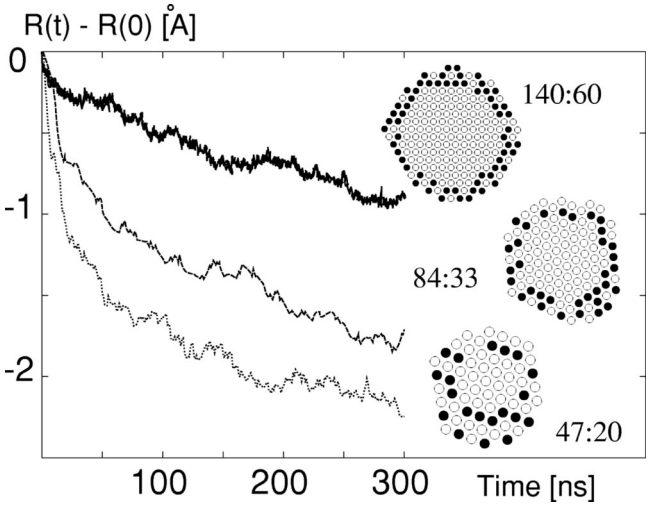


FIG. 3. Comparison of time dependence of the mean distance $R(t)$ for the three different sizes of binary clusters $A_{47}B_{20}$, $A_{84}B_{33}$, and $A_{140}B_{60}$ together with their snapshots of the configuration taken at $t = 300$ ns. Note that the vertical axis is $R(t) - R(0)$.

is often used to quantify the mobility of the whole cluster atoms.

## III. NUMERICAL RESULTS

### A. How rapid is the alloying in smaller sized clusters?

One of the most surprising results of the alloying process in the nanosized metallic clusters is that the alloying time is much shorter than that of the bulk medium. This fact implies that the diffusion rate of the atoms into the cluster depends sensitively on the size of the cluster. First of all, we demonstrate that our isothermal simulation certainly reproduces the size-dependent effect. In the present paper, we do not investigate the detailed features of the size-dependence problem, which will be discussed in detail in a subsequent paper. The aim of this section is only to show the validity of our modeling and of our method of simulation in connection with the size-dependence problem.

Figure 3 compares the time dependence of the mean distance $R(t)$ for the three different size of binary clusters $A_{47}B_{20}$, $A_{84}B_{33}$, and $A_{140}B_{60}$ together with their snapshots of the configuration taken at $t = 300$ ns starting from the initial configuration shown in Fig. 2. Here we choose $\alpha = 1.2$, which is the typical value used in the present paper, and the temperature is controlled to $T = 600$ K by the averaged kinetic temperature scaling algorithm.

When we compare the alloying dynamics in different size of clusters, the composition of the two atomic species must be taken so that the decrease of the potential energy per atom in the ideally alloyed limit, which is given by $\Delta U/(N_A + N_B) = \epsilon(\alpha - 1) r(1-r) z$, may be the same for all different sizes. Thus the ratio of composition $r = N_B/(N_A + N_B)$ must be chosen a common value ($r \sim 0.3$ in the present case) in all the different size of clusters to be compared.

As is evident from the figures, the velocity of guest atoms placed initially on the surface to diffuse inside the cluster, which is characterized by $dR(t)/dt$, decreases markedly as the size of the cluster increases. Such observations are the strong evidence that the essential origin of the very rapid

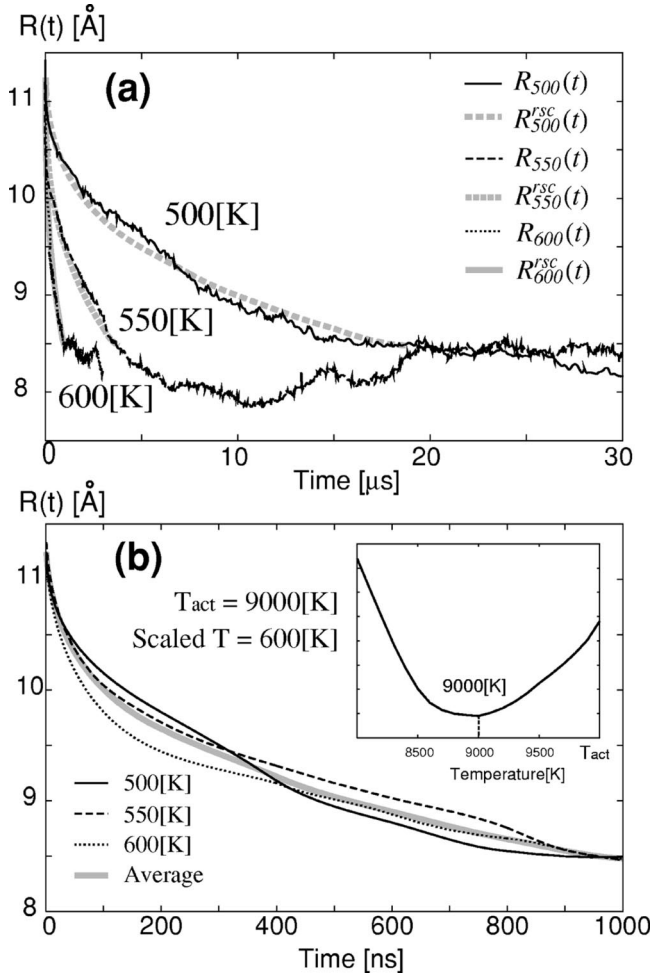


FIG. 4. Time dependence of mean distance of guest atoms $R(t)$ from the center. (a) Black lines are the data of the $\alpha=1.0$ cluster at $T=500,550,600$ K and gray lines are the averaged optimally scaled data rescaled back to the individual temperatures $T$ of original data, namely, $R^{*sc}(te^{T_{act}(1/T-1/600)})$ (b) Black lines are $R(t)$'s at 500 K, 550 K, and 600 K, all of which are Arrhenius scaled at $T_{scale}=600$ K. Gray line is the average of all the black lines, ie., $R^{*sc}(t)$. The insertion indicates $D(T_{act})$ vs $T_{act}$.

alloying is the smallness of the cluster size. To clarify the physical mechanism of such a very rapid process, we make detailed quantitative analyses for the diffusion process into the cluster. Similar analysis has been done in the previous paper, but the results are quantitatively very unsatisfactory because of the temperature rise during the alloying process.

### B. Radial diffusion and alloying

#### *1. Diffusion*

The results demonstrated in the preceding section imply the presence of a very rapid diffusion process in the radial direction of small clusters. As will be described below, such a rapid diffusion process is by no means peculiar to the binary clusters with negative heat of solution, but exists in small homogeneous clusters composed of only a single atomic species. We therefore start our investigation with the radial diffusion process, which can be quantitatively captured by the mean distance $R(t)$, taking the homogeneous clusters as the reference system.

Figure 4(a) shows the time series of $R(t)$ obtained for $A_{47}B_{20}$ at the three different temperatures $T=500$, 550, 600 well below $T_M\sim 700$–750 K. These data indicate that the diffusion process very sensitively depends on temperature. At every increase of 50 K the time for the guest atoms to penetrate fully into the cluster to becomes 3–4 times shorter, which implies that the radial diffusion process is effectively described by an Arrhenius-like activation process.[17]

We have taken an ensemble average over more than 100 samples for each data (note that each sample contains $N_B=20$ atoms and so the total number of sampled trajectories is more than 2000), but the fluctuation around the ensemble averaged $R(t)$ is not still negligible. Such an anomalous fluctuation is a remarkable characteristic of a small cluster and is of great interest by itself, but it prevents us from knowing the ''representative'' behavior of $R(t)$ at each temperature. To extract precise information of activation process from such an anomalously fluctuating data, we use the following method.

Suppose that the time series $y=f_i(t)$ measured at a fixed temperature $T_i$ represent an Arrhenius-like activation process characterized by a unique time scale $\tau_c$ of activation type, then the data taken at different temperatures $T_i(1\leqslant i\leqslant M)$ should coincide with each other upon the scale transformation

$$f^{sc}_{T_{act},i}(t)\equiv f_i\left(t\exp\left[T_{act}\left(\frac{1}{T_{scale}}-\frac{1}{T_i}\right)\right]\right), \tag{18}$$

where $T_{scale}$ is an arbitrary temperature. We call the scale transformation defined by the right-hand-side of Eq. (18) the *Arrhenius scaling* at $T_{scale}$ upon the activation temperature $T_{act}$. If all the data are Arrhenius scaled upon an activation temperature $T_{act}$ coincide with each other, we say that the data is *Arrhenius scalable.*

The radial diffusion data are not rigorously Arrhenius scalable by a single time scale characterized by a particular activation temperature. (see Sec. III D). But if we limit the time range of observation to the most active period of the radial diffusion such that $f_{mn}\leqslant y=f_i(t)\leqslant f_{mx}$, where $f_{mn}$ and $f_{mx}$ are common bounds of the window covering the most active period of the process $y=f_i(t)$, we can decide the optimal activation temperature $T^*_{act}$ as the $T_{act}$ minimizing the maximum distance defined by

$$D(T_{act})\equiv \max_{i\neq j}\int_{f_{mn}}^{f_{mx}}\left|f^{sc}_{T_{act},i}{}^{-1}(y)-f^{sc}_{T_{act},j}{}^{-1}(y)\right|dy, \tag{19}$$

for a set of Arrhenius-scaled data obtained at different temperatures, where $f^{sc}_{T_{act},i}{}^{-1}(y)$ indicates the inverse function of $y=f^{sc}_{T_{act},i}(t)$. We further define *the averaged optimally scaled time series* as the average over the optimally Arrhenius-scaled data

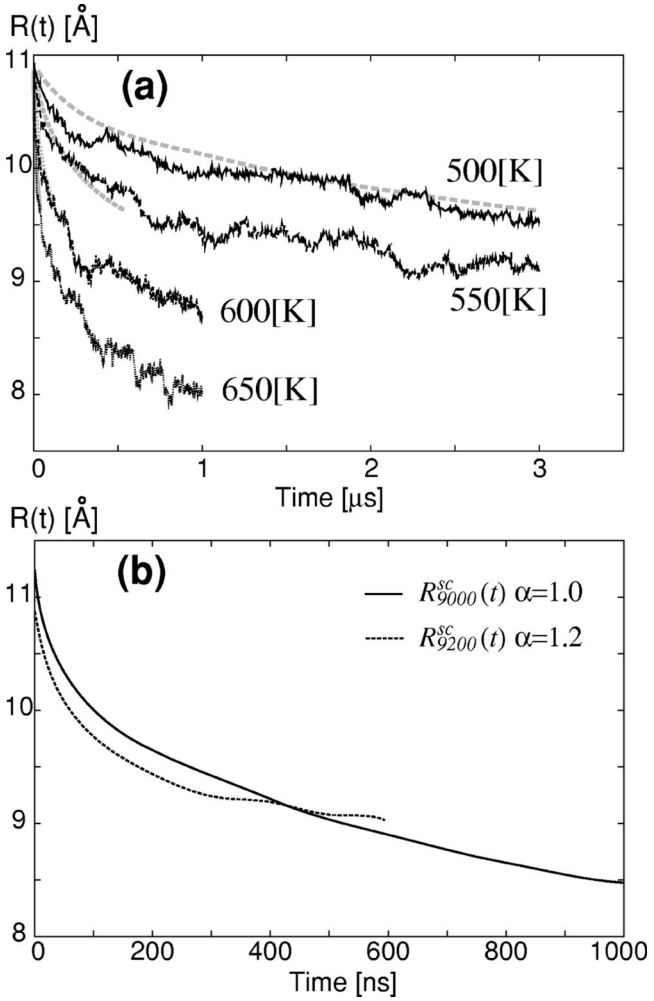


FIG. 5. Time dependence of mean distance of guest atoms $R(t)$ for the $\alpha=1.2$ cluster. (a) Black lines are $R(t)$ at $T=500,550,600$, and 650 K, while gray lines are the averaged optimally Arrhenius-scaled data rescaled back to each original temperature, i.e., $R^{*sc}(te^{T_{act}(1/T-1/600)})$ Each set of black and gray lines coincide very well. (b) The optimally Arrhenius-scaled $R(t)$ of $\alpha=1.2$ (dotted line) is compared with that of $\alpha=1.0$ (solid line), where $T_{scale}$ is chosen at 600 K.

$$f^{*sc}(t)\equiv f^{sc}_{T^*_{act}}(t)=\sum_{i=1}^{M}\frac{f^{sc}_{T^*_{act},i}(t)}{M}. \tag{20}$$

We hereafter omit the superscript * from $T^*_{act}$ when there is no other any confusion.

As demonstrated in the inset of Fig. 4(b), we can decide the value of the optimal activation temperature $T_{act}=9000\pm500$ K, according to the method mentioned above. The three data in Fig. 4(a) are Arrhenius-scaled data with respect to the optimal activation temperature $T_{act}$ and depicted in Fig. 4(b), where the temperature $T_{scale}$ is chosen at 600 K. Beside them the averaged data $R^{*sc}(t)$ is also depicted, and agreement of them seems to be satisfactory. To make a further check, we rescale the averaged data back to the individual original temperature to obtain $R^{*sc}(te^{T_{act}(1/T_i-1/T_{scale})})$ [the inverse transformation of Eq. (18)]. They are compared with the original data $R_i(t)$ in Fig. 4(a). The agreement seems to be excellent and we may conclude that the radial diffusion is dominated by an effective activation process at least in the active stage of diffusion.

Next, we discuss the radial diffusion process of the binary cluster with $\alpha=1.2$, i.e., the case of negative heat of solution. $R_i(t)$ measured at the four temperatures $T_i=500$, 550, 600, 650 K are depicted in Fig. 5(a). The optimal Arrhenius scaling was applied to these data, and we evaluated the optimum value of the activation temperature $T_{act}=9200\pm500$ K. The averaged optimally scaled time series $R^{*sc}(te^{T_{act}(1/T_i-1/T_{scale})})$ are also depicted and compared with the original data. The fact that they exhibit a satisfactory agreement with the actual data means that the diffusion process of the binary cluster is also described by an effective activation process.

A nontrivial and somewhat unexpected conclusion is that within the permissible error the activation temperature of the radial diffusion agrees with the activation temperature of the homogeneous cluster. We compare in Fig. 5(b) the averaged optimally scaled time series $R^{*sc}(t)$ of the binary $\alpha=1.2$ cluster with that of the $\alpha=1.0$ cluster. They are both scaled at $T_{scale}=600$ K assuming the common optimal activation temperature $T_{act}=9000$ K. It is evident that the time scales of the penetration process do not differ in the two cases. From these observations we have the following conclusion:

*The guest atoms obeys an Arrhenius-type diffusion process of the effective activation temperature of* $T_{act}=9000\pm500$ K. *The activation temperature does not depends upon* $\alpha$. *More precisely, the diffusion velocity does not significantly depend upon* $\alpha$ *at the same temperature*.

This is an important result implying that the rapid diffusion is a common dynamical feature of small clusters and is by no means peculiar to binary clusters.

At first sight such a result seems to sharply contradict with the experimental observation that the heat of solution is the driving force of the spontaneous alloying process. However, the mean distance does not suitably quantify the degree of alloying, as is discussed in Sec. II D.

#### *2. Alloying*

As is discussed in Sec. II D, a physical quantity that measures the degree of alloying is the bonding number $n_B(t)$ introduced by Eq. (13). If $\alpha>1$, the increment in $n_B(t)$ is proportional to the decrement in the potential energy, which measures how the energetically preferable mixing of the guest atoms with the host atoms is accomplished. We show in Fig. 6(a) the time evolution of $n_B(t)$ observed in the homogeneous cluster at $T=500$, 550, 600 K On the other hand, Fig. 6(b) depicts $n_B(t)$ in the binary cluster ($\alpha=1.2$) at the four temperatures $T=500$, 550, 600, 650 K.

The guest atoms initially on the surface of cluster enter into the inside of the cluster because they energetically prefer to increase the bond number with different species of atoms, thereby decreasing the total *enthalpy* (or the total potential energy). Thus, as in Fig. 6(b), the bond number $n_B(t)$, in general, increases monotonously and approach the ideal value of alloying $n^c_B=z(1-r)=4.2$ in case of the binary

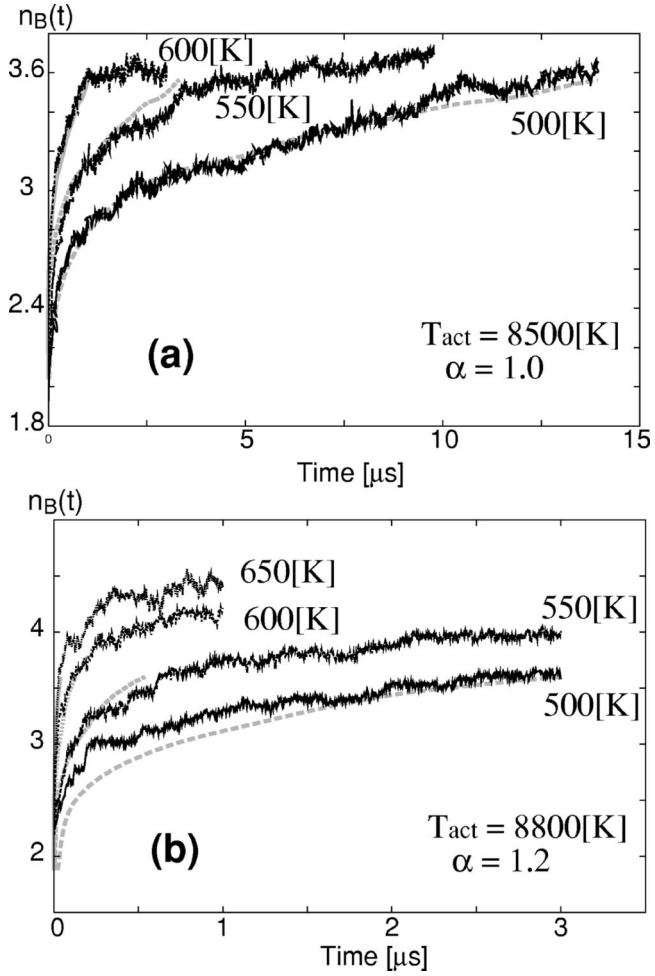


FIG. 6. Time dependence of the bond number $n_B(t)$. (a) Black lines indicates $n_B(t)$ of the $\alpha=1.0$ cluster at $T=500$, 550, and 600 K. Gray lines are the optimally Arrhenius-scaled data rescaled back to each original temperature $T$, i.e., $n_B^{*sc}(te^{T_{act}(1/T-1/600)})$, (b) black lines are $n_B(t)$ of the $\alpha=1.2$ cluster at $T=500$, 550, 600, and 650 K. Gray lines are the optimally Arrhenius-scaled data $n_B^{*sc}(te^{T_{act}(1/T-1/600)})$.

clusters with negative heat of solution ($\alpha>1$). As in Fig. 6(a), $n_B(t)$ increases also in the homogeneous cluster with $\alpha=1.0$ in which no net change of enthalpy occurs. In this case the *entropy* effect, which is not negligible compared with the enthalpy at a finite temperature, may be considered as the emotional force.

It is evident that the growth rate of $n_B(t)$ is much faster in the binary cluster than in the homogeneous cluster if the temperature is same, and the negative heat of solution indeed plays a key role in the rapid growing process of $n_B(t)$, which makes a sharp contrast to the case of $R(t)$.

In spite of such a remarkable effect of the heat of solution, it does not give a significant effect on the activation process of the alloying. Indeed, we estimate the activation temperature by the method of optimal Arrhenius scaling, assuming that the time evolution of $n_B(t)$ obeys an Arrhenius-like activation process. We obtain $T_{act}=8500\pm500$ K and $T_{act}=8800\pm500$ K for the homogeneous and binary clusters, respectively. We show in Fig. 7(a) the smoothed time series

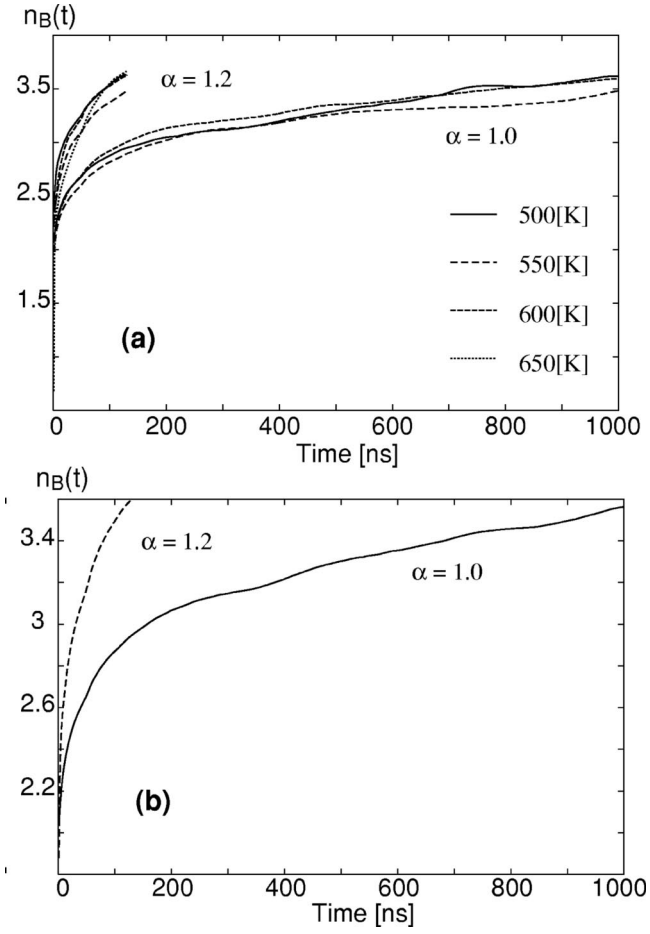


FIG. 7. Comparison of the optimally Arrhenius scaled $n_B(t)$ for $\alpha=1.0$ and $\alpha=1.2$ clusters. (a) The data $n_B^{sc}(t)$ obtained at various temperatures (500, 550, 600 K for the $\alpha=1.0$ cluster,and 500, 550, 600, 650 K for the $\alpha=1.2$ cluster) optimally Arrhenius scaled at $T_{scale}=600$ K. (b) The *averaged* optimally Arrhenius scaled $n_B^{*sc}(t)$ for the $\alpha=1.0$ and $\alpha=1.2$ clusters, where $T_{scale}=600$ K.

of $n_B(t)$ obtained at various temperatures for the binary cluster of $\alpha=1.2$ and those for the homogeneous cluster, namely, $n_{BT_{act},i}^{sc}(t)$. Their original data are those depicted in Figs. 6(a) and 6(b). They are all smoothed and Arrhenius-scaled data to the common temperature $T_{scale}=600$ K based upon the activation temperature $T_{act}=8700$ K, which is the mean value of the optimal activation temperatures of $\alpha=1.0$ and $\alpha=1.2$. The scaled time series of $\alpha=1.2$ and those of $\alpha=1.0$, respectively, get close together and almost overlap with each other, which strongly indicates that the Arrhenius scaling works very well.

The optimal activation temperatures are consistent with those decided by the mean distance $R(t)$ in the preceding section. Again we have to conclude that both $R(t)$ and $n_B(t)$ are dominated by the same activation process with the effective activation temperature $T_{act}=8500$ K–9000 K, which is insensitive to the heat of solution. Hereafter, it is denoted by $T_\perp$.

Although the heat of solution does not significantly affect on the activation temperature, which dominates the SA, it plays a very significant role in the alloying process. Indeed,

Fig. 7(a) indicates that $n_B(t)$ of $\alpha=1.2$ increases much more rapidly than those of $\alpha=1.0$. To demonstrate such a difference more clearly, we show in Fig. 7(b) the averaged optimally scaled time series $n_B^{*sc}(t)$, which are obtained by averaging the data depicted in Fig. 7(a) according to Eq. (20). They are the counterparts of Fig. 5(b) and represent ''typical'' functional forms of $n_B(t)$ for $\alpha=1.0$ and $\alpha=1.2$, which are extracted from the behaviors at various temperatures. We regard the growth rate $|dn_B^{*sc}(t)/dt|$ as the function of $n_B$ $[=n_B^{sc}(t)]$ rather than as the function of $t$. Then the growth rate, in general, decreases as $n_B$ approaches the value of the ideal alloying $n_B^c=z(1-r)=4.2$. The ratio of the growth rate of $\alpha=1.2$ to that of $\alpha=1.0$ is more than eight times in the active stage of the alloying process and the ratio is further enhanced as the alloying proceeds.

At first sight, it sounds strange that such a remarkable difference exists between $R(t)$ and $n_B(t)$ although the activation temperatures of them coincide. It should be stressed again that the ''diffusion'' does not mean the ''alloying'': $n_B(t)$ measures the number of bonding of the guest atoms with the host atoms, and $R(t)$ is the mean distance of the guest atoms from the center of the cluster. In the case of homogeneous cluster, the guest atoms diffuses deeply inside, but they are clustered and are not well mixed with the host atoms when its mean distance $R(t)$ takes the same value as $R(t)$ of the binary cluster.

We can introduce the alloying time $t_{alloy}$ that characterizes the time scale of alloying by using $n_B(t)$. We define $t_{alloy}$ as the time at which $n_B(t)$ reaches the mean value of $n_B$ in the initial stage and $n_B$ in the ideally alloyed stage

$$n_B(t=t_{alloy})=[n_B(t=0)+n_B^c]/2. \tag{21}$$

The observations of Fig. 6 and Fig. 7 allow us to summarize as follows:

The temperature dependence of the alloying time is of the Arrhenius type with the activation temperature $T_\perp=9000\pm500$ K, which is insensitive to the negative heat of solution. The effect of negative heat of solution is taken into account in the form of a preexponential factor $\nu=\nu(\alpha-1)$,

$$t_{alloy}=\nu(\alpha-1)e^{T_\perp/T}. \tag{22}$$

The conclusion is rather surprising and is unexpected from the results of microcanonical simulation.[17] It is settled for the first time by controlling the temperature at a desired accurate level. The $\alpha$ dependence of the pre-factor is discussed in more detail in Sec. III C.

### C. Surface activity and radial diffusion

#### 1. Surface diffusion

What is the mechanism of the very fast diffusion into the cluster? Diffusion in bulk media is initiated by vacancies or interstitial effect.[20,29,30] However, such mechanisms are not relevant in microclusters. From an energetical argument, it can be shown that the possibility of vacancies formation inside the clusters much reduces as its radius becomes less than a characteristic size.[31] Indeed, observing animations of our simulation, creation of vacancies inside the cluster was a very rare event even at the temperature close to the melting point. Further, we cannot find any evidence that the interstitial deformation of crystal lattice, which allows an atom to penetrate into inner layers, takes place inside the cluster. Therefore, neither of them is responsible for the very rapid diffusion into the cluster. We thus have concluded that the dominant mechanism of the radial diffusion is not the defect formation in the inner layers of the cluster.

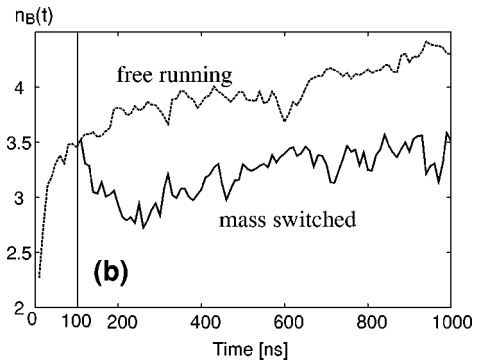


FIG. 8. Time dependence of $n_B(t)$ for the free running and the mass switching simulation. In the latter simulation the mass of the surface atoms was switched to 300 times larger one at $t_s=100$ ns, which is indicated by a vertical line. $A_{47}B_{20}$-cluster is used, where $T=600$ K and $\alpha=1.2$

On the other hand, it is well known that the atoms of the cluster can move very actively along the surface,[14,32–34] and it is plausible to suppose that the surface activity will play a key role in the spontaneous alloying and the rapid radial diffusion. In this subsection we investigate activity of atoms on the surface of the cluster.

It is easy to measure the diffusion rate of atoms along the surface, but a more fundamental quantity which measures the surface activity is the accumulated distance index $S(t)$ defined by Eq. (17). Most of the rearranging events of atoms contributing to $S(t)$ occur on the outermost layer closest to the surface,[16,17,34] and so the distance index per unit time $dS(t)/dt$ is proportional to the probability of an atom to change its lattice site along the surface and is thus proportional to the surface diffusion rate, which is also confirmed numerically. We can decide the activation temperature associated with the surface activity by applying the optimal Arrhenius scaling to the data of $S(t)$. We denote the activation temperature by $T_\parallel$ hereafter.

It is estimated at $T_{act}=4100\pm100$ K and is less than 1/2 of the radial activation temperature $T_\perp\sim9000\pm500$ K. It is convenient to represent the activation energies in terms of the energy per unit bond $\epsilon/k_B=3980$ K,

$$k_BT_\parallel/\epsilon\sim1.03,\quad k_BT_\perp/\epsilon\sim2.3\pm0.1. \tag{23}$$

#### 2. Mass switching experiment

To confirm the key role of the surface, we show a simulation demonstrating how the alloying process is affected if the motion along the surface is interrupted by an artificial operation.

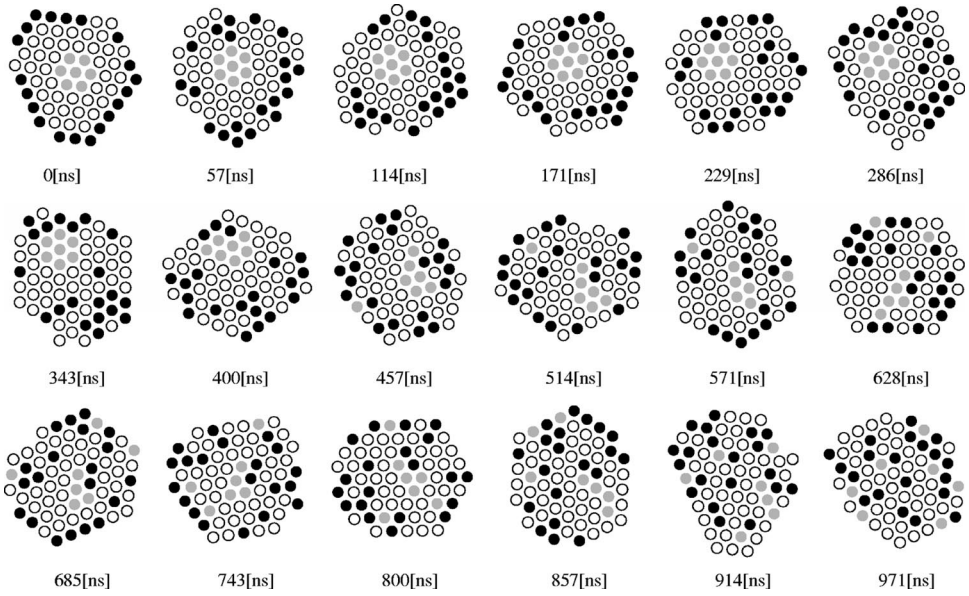


FIG. 9. Snapshots of the alloying process for the cluster $A_{47}B_{20}$ of $\alpha=1.0$, at $T=600$ K. The virtual guest atoms initally located near the surface are denoted by black circles, while the gray circles are virtual host atoms forming the core of the cluster at $t=0$.

We start the simulation of alloying from similar initial configurations as shown in Fig. 2, but the mass of some atoms on the surface are switched to a larger mass (typically 300 times larger one) at a certain time $t=t_s$ when about half of the guest atoms initially on the surface are absorbed into layers inner than the outermost layer. The atoms whose mass is changed are selected from the host atoms in the outermost layer, and so no guest atoms contributing to the alloying undergo the mass switching. Sudden increase of the mass of atoms decrease their frequencies of vibration, thereby playing the role of the stoppers for the motion of guest atoms along outermost layer on the surface. We are interested in how further penetration of guest atoms into the inner layers is modified afterwards. The simulation was done by using the $A_{47}B_{20}$ cluster with $\alpha=1.2$ at $T=600$ K, where mass of the selected surface atoms was switched to 300 times larger one at $t_s=100$ ns. We show in Fig. 8 the time evolution of bond number $n_B(t)$ in comparison with that of the free running simulation. It is evident that the growth of $n_B(t)$ is notably suppressed and keeps almost the same level at $t=t_s$, although $n_B(t)$ of the free running simulation increases above the value of ideal mixing. The above observation provides a direct evidence that any event which occur inside the cluster is not responsible for the radial motion and the presence of the surface plays the key role in the rapid alloying process.

### *3. On the mechanism of radial diffusion*

Then how the active motion along the surface is converted into the rapid radial motion? Since the radial diffusion rate does not significantly depend on $\alpha$, we consider the homogeneous cluster ($\alpha=1.0$) for the sake of simplicity. Therefore, there is no temperature rise and the alloying occurs in the equilibrium.

A 2D microcluster almost takes the form of a hexagon whose surface is composed of six edges and six corners in the equilibrium. Some atoms are on the outermost layer and they move very rapidly from site to site along the surface. They move collectively forming a group of an appropriate number (typically three atoms) so as to reduce the number of steps on the surface. The activation energy for a surface atom to change their site along the edge can be evaluated as $T_{act}\sim 1800$ K, which is much less than $T_{\parallel}\sim 4100$ K, and so $T_{\parallel}$ should be associated with the activation energy of the collective motion.

Owing to the active movement along the surface, most of the atoms covering an edge may migrate to other edges. Then the atoms contained in the edge are exposed, and they form the outermost layer. As long as the newly exposed edge is filled with atoms, it is still inactive. But if atoms are removed from the new edge, it gains the surface activity. The easiest way to remove an atom from the newly exposed edge is to move the atom sited on the corner (i.e.,end of the edge) to the next edge. Once the corner atom is moved, the next atom on the new edge can migrate to other edges more easily. In such a way the newly exposed edge has vacancies and gains surface activity, and most of the atoms in the new edge have the chance to migrate to other edges along the surface. Then the inner layer is exposed and again has the chance to gain surface activity. On the other hand, the edges newly covered by the atoms migrating from the newly exposed edge are buried in them to lose the surface activity. Repetition of such exposing and burying processes enables the inner atoms to come out to the surface. Conversely speaking, the surface atoms are allowed to enter into the cluster and to exchange their original positions with the inner atoms. This is just the diffusion process governed by the activation temperature $T_{\perp}$.[35]

We show in Fig. 9 a series of snapshots manifesting what is taking place according to the scenario described above. We particularly focus our attention to the seven atoms colored by gray, which form the core part of the cluster at $t=0$. They are pushed to reach close to the surface of the cluster at $t\sim 400$ ns. The core atoms move in a group forming a solid object until they come close to the surface. On the other hand, the atoms which are initially sited on the surface and encircling the cluster almost symmetrically become distrib-

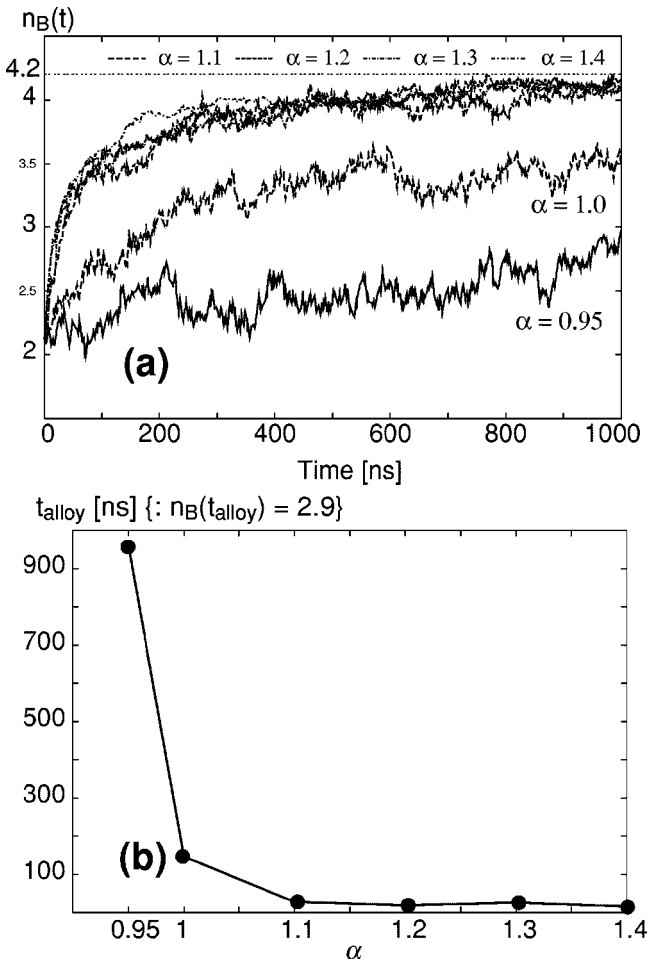


FIG. 10. (a) Time dependence of $n_B(t)$ at various values of $\alpha$. (b) The dependence of the alloying time on $\alpha$ for $A_{47}B_{20}$ cluster at $T=600$ K.

uted at random in the inner part of the cluster unoccupied by the gray atoms. Such a kind of the motions correspond to the radial diffusive motion of the surface atoms. An atom is taken away from the group of core atoms when they come close to the surface ($t\sim 400$ ns). They are pushed back into the inner layers of the cluster ($t\sim 460$ ns) and again approach the surface ($t\sim 510$ ns), when an atom is taken away from the group ($t\sim 570$ ns). After repeating such processes, the object composed of the core atoms, which is moving as if a solid body inside the cluster, is damaged as it comes close to the surface and loses its original form after a lapse of sufficiently long time: all the constituent atoms are scattered at random over the cluster ($t\sim 900$ ns).

The key processes of the rapid radial diffusion are the *exposure* or the *burying* of an edge, which is caused by the migration of the atoms along the surface. As discussed above, the newly exposed edge will be activated by moving the atom on the corner. The process requires the atom to cut two bonds on the way from the corner to the next edge, which result into the activation energy of approximately $2\epsilon/k_B\sim 8000$ K. On the other hand, the burying of an old edge will be dominated by the process of carrying an atom absorbed at an end of the outermost layer (i.e., the step) onto it. The associated activation energy is also estimated approximately at $2\epsilon/k_B\sim 8000$ K. These estimations are very crude and are significantly less than $T_\perp\sim 2.3\epsilon/k_B$. Moreover, quite recently, there have been some evidences that more complicated collective motions dominate the exposure and burying process. In anyway, more qualitatively accurate analyses are required to identify the true rate-limiting process, but it is sure that the precise evaluation of $T_\perp$ presented in our paper provides with very useful information about the dominant process which converts the surface activity into the rapid radial motion.

Finally we comment that the transport process described here is observed also for the clusters modeled by a many-body binding force.[28]

### D. Dependence of alloying process upon heat of solution

As has been stressed, the negative heat of solution is a key parameter in the experiments of SA. It does not significantly influence the radial diffusion rate, but it drastically enhances the alloying rate.

Figure 10(a) shows the time evolution of bond number $n_B(t)$ of the alloying process for binary clusters $A_{47}B_{20}$ with various values of $\alpha$. Figure 10(b) depicts the alloying time evaluated by the data of (a) as the function of $\alpha$. A remarkable fact is that the alloying time decreases suddenly as $\alpha$ increases but it saturates beyond $\alpha\sim 1.1$.

The saturation is comprehensible by considering the formation of alloyed structure in the later stage of alloying process. Suppose that $\alpha>1$, then as the guest atoms penetrate inside the cluster, they are mixed properly with the host atoms so as to reduce the total potential energy to form an alloyed structure. The alloyed structure is more stable than the structure composed of the host atoms alone, and will suppress the activity on the surface.

To evaluate more quantitatively the relation between activity and alloying, we consider the final stage of alloying process in which all the guest atoms are mixed ideally with the host atoms. In such an ideal situation, the mean coupling strength per unit bond $\epsilon_{eff}$ is evaluated by equating the total potential energy $-Nz\epsilon/2+Nrz(1-r)\epsilon$ of the alloyed cluster (nearest-neighbor approximation) to the effective total potential energy $-Nz\epsilon_{eff}/2$, which yields

$$\epsilon_{eff}=\epsilon\{1+2r(1-r)(\alpha-1)\}. \tag{24}$$

Increase in the effective coupling strength will enhance various activation temperatures such as $T_\parallel$ and $T_\perp$. In fact, if we suppose that the ideally alloyed binary cluster may be approximated by a homogeneous cluster of the effective interaction strength $\epsilon_{eff}$, a simple scaling argument for our model equation results in the enhancement of the activation temperature

$$T_{act,eff}=\frac{\epsilon_{eff}}{\epsilon}T_{act}=\{1+2r(1-r)(\alpha-1)\}T_{act}. \tag{25}$$

For example, in case of the $A_{47}B_{20}$ cluster with $\alpha=1.5$ and $r=N_B/(N_A+N_B)=0.3$ $T_{act,eff}$ enhances $\sim 20\%$, which will cancel the decrease of $t_{alloy}$ described by the prefactor $\nu(\alpha$

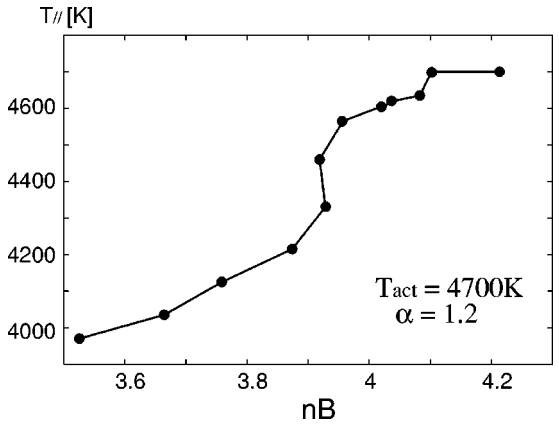


FIG. 11. $n_B$ vs $T_\parallel$ for the $A_{47}B_{20}$ cluster ($\alpha=1.2$). $T_\parallel$ is decided as the function of $n_B$ by using the data of $dS/dt$ at four different values of temperature $T=500$, 550, 600 K and 650 K when each $n_B(t)$ reaches a common value $n_B$.

$-1$). In the actual process of alloying, the rise of $T_{act}$ occurs slowly in time in accordance with the evolution of alloying. In Fig. 11, we show a numerical evidence manifesting the gradual increase of $T_\parallel$ as the function of bond number $n_B$, which is just the parameter measuring how the alloying is achieved (see Table I).

Here we give the summary of the present subsection as follows:

The prefactor of $\nu$ of the alloying time $t_{alloy}$ decreases steeply as $\alpha$ increases across $\alpha=1.0$, but the decrease of $t_{alloy}$ soon saturates because of the formation of a stable alloyed structure.

At first sight such a result may give an impression that it is inconsistent with the experimental result that the negative heat of solution is the decisive factor controlling SA. However, considering that the experiments have been done for the combination of atomic species with $\alpha<1.1$, the rapid decrease of the alloying time close to $\alpha=1$ corresponds to the experimental observations.

## IV. CONCLUSIONS AND DISCUSSIONS

In the present paper, the dynamical process of the diffusion associated with the spontaneous alloying in 2D binary clusters is investigated in detail by using a deterministic algorithm which can control the time average of kinetic temperature without modifying the Newton's equation of motion very significantly. The microcanonical simulation of the spontaneous alloying was first presented by Shimizu *et al.*,[16,17] but in their simulation the heating up of the cluster due to the emission of reaction heat makes it difficult to decide the precise dependence of the alloying process on temperature, heat of solution, and the cluster size etc. In the present work the raise of temperature in the alloying process is entirely removed and the precise dependence of the alloying process on the temperature ($T$) and the negative heat of solution ($\alpha-1$) is clarified for a cluster of typical size.

The results elucidated in the present paper are summarized as follows:

TABLE I. Numerically estimated several kinds of activation temperatures for the homogeneous and the binary clusters.

| | $\alpha=1.0$ | | $\alpha=1.2$ |
|---|---|---|---|
| $T_\parallel$ | $4100\pm100$ K | | $4000\rightarrow4700\pm100$ K[a] |
| $T_\perp$ | | $9000\pm500$ K[b] | |
| $T_C$ | $12000\pm1000$ K[c] | | |

[a]In the initial stage $T_{act}$ is 4000 K, and rises gradually up to 4700 K (see Fig. 11).

[b]$T_\perp of \alpha=1.2$ is slightly higher than $T_\perp of \alpha=1.0$.

[c]As an additional information, the activation temperature $T_C$ of the mean square displacement of the atom initially located at the center of the cluster is also shown. See Sec. III C 3.

(1) The major part of the diffusion process of the guest atoms into the cluster obeys the Arrhenius law, and the activation temperature is decided by the optimal Arrhenius scaling. We could not found the evidence that the activation temperature associated with the diffusion rate does significantly depend upon the heat of solution.

(2) The alloying rate, however, exhibits a different behavior from the diffusion rate and depends remarkably upon the negative heat of solution. We showed that the effect of the negative heat of solution on the alloying rate appears as the preexponential factor of the Arrhenius-like behavior whose activation temperature is the same as that of diffusion process and thus is insensitive to the negative heat of solution.

(3) A slight increase in the negative heat of solution makes the alloying rate increase very steeply, which agrees with the experimental results, but a further increase makes the alloying rate saturate. The origin of the saturation mechanism is discussed in connection with the formation of a stable alloyed structure. The fact that the activation temperature do not significantly depends upon the negative heat of solution means that the basic process dominating the very rapid diffusion into the cluster is a universal feature of microclusters.

We also showed a direct evidence that the surface activity controls the rapid radial diffusion, and we discussed rather in detail the mechanism with which the surface activity is converted into the rapid radial diffusion. A more quantitative analysis for the mechanism will be discussed in fully detail in a forthcoming paper.

The present paper has succeeded in establishing precise dependence of the alloying process on temperature and negative heat of solution for clusters of a typical size. In the present paper, we also showed a clear evidence that the diffusion process is drastically suppressed as the cluster size increases, but we did not show systematic analyses for the size effect. The subsequent paper will be devoted to elucidating the size effect.

## ACKNOWLEDGMENTS

The authors are very grateful to H. Yasuda for useful discussions. The authors also thank much to S. Tsuji for his hospitality of serving his country house as our institute in which some key ideas in the present article have been developed.

*Electronic address: tkoba@ike-dyn.ritsumei.ac.jp
†Electronic address: ahoo@ike-dyn.ritsumei.ac.jp

[1] H. Yasuda, H. Mori, M. Komatsu, K. Takeda, and H. Fujita, J. Electron Microsc. **41**, 267 (1992).
[2] S. Sugano and H. Koizumi, *Microcluster Physics*, 2nd ed. (Springer, New York, 1999), iSBN 3 540 63974 8.
[3] S. Iijima and T. Ichihashi, Phys. Rev. Lett. **56**, 616 (1986).
[4] P.M. Ajayan and L.D. Marks, Phys. Rev. Lett. **60**, 585 (1988).
[5] P.M. Ajayan and L.D. Marks, Phys. Rev. Lett. **63**, 279 (1989).
[6] S. Sawada and S. Sugano, Z. Phys. D: At., Mol. Clusters **14**, 247 (1989).
[7] S. Sawada and S. Sugano, Z. Phys. D: At., Mol. Clusters **20**, 258 (1991).
[8] S. Sawada and S. Sugano, Z. Phys. D: At., Mol. Clusters **24**, 377 (1992).
[9] K. Ikeda, K. Otsuka, and K. Matsumoto, Suppl. Prog. Theor. Phys. **99**, 295 (1989).
[10] I. Tsuda, World Feature **31**, 105 (1991).
[11] K. Kaneko, Physica D **41**, 137 (1990).
[12] H.L. Davis, J. Jellinek, and R.S. Berry, J. Chem. Phys. **86**, 6456 (1987).
[13] C.L. Briant and J.J. Burton, J. Chem. Phys. **63**, 2045 (1975).
[14] V. Nauchitel and A. Pertsin, Mol. Phys. **40**, 1341 (1980).
[15] Y. Kimura, Y. Saito, T. Nakada, and C. Kaito, Phys. Low-Dimens. Semicond. Struct. **1/2**, 1 (2000).
[16] Y. Shimizu, S. Sawada, and K. Ikeda, Eur. Phys. J. D **4**, 365 (1998).
[17] Y. Shimizu, K.S. Ikeda, and S.I. Sawada, Phys. Rev. B **64**, 075412 (2001).
[18] H. Mori, H. Yasuda, and T. Kamino, Philos. Mag. Lett. **69**, 279 (1994).
[19] H. Yasuda and H. Mori (private communication).
[20] P. G. Shewmon, *Diffusion in Solids* (McGraw-Hill, New York, 1963).
[21] S. Nosé, Mol. Phys. **52**, 255 (1984).
[22] W.G. Hoover, Phys. Rev. A **31**, 1695 (1985).
[23] W.F. van Gunsteren and H.J.C. Berendsen, Mol. Phys. **45**, 637 (1982).
[24] S.M. Kast, K. Nicklas, H.-J. Baer, and J. Brickmann, J. Chem. Phys. **100**, 566 (1994), the stochastic collision constant-temperature MD method.
[25] S.M. Kast and J. Brickmann, J. Chem. Phys. **104**, 3732 (1996), the stochastic collision constant-temperature MD method.
[26] T. R. Kobayashi, K. S. Ikeda, S. Shimizu, and S. Sawada (unpublished).
[27] L. Girifalco and V. Weizer, Phys. Rev. **114**, 687 (1959).
[28] S. I. Sawada, Y. Shimizu, and K. S. Ikeda, Phys. Rev. B (to be published).
[29] L. A. Girifalco, *Atomic Migration in Crystals* (Blaisdell, Naltham, 1964).
[30] P. Guiraldenq, *Diffusion dans les Mètaux* (Techniques de l'ingenieux, Paris, 1978).
[31] E. Fujita, J. Jpn. Inst. Met. **30**, 322 (1966).
[32] R. Kofman, P. Cheyssac, A. Aouaj, Y. Lereah, G. Deutscher, T. Ben-David, J. Penisson, and A. Bourret, Surf. Sci. **303**, 203 (1994).
[33] R. Kofman, Eur. Phys. J. D **9**, 441 (1999).
[34] H. Cheng and R.S. Berry, Phys. Rev. A **45**, 7969 (1992).
[35] In the preparation of the present paper, one of the referee point out the similarity of our mechanism with the circular diffusion (or periphery diffusion) reported in, for example, in J.-M. Wen, Phys. Rev. Lett. **73**, 2591 (1994); D.S. Sholl and R.T. Skodje, *ibid.* **75**, 3158 (1995); S.C. Wang, *ibid.* **81**, 4923 (1998). The evaporation-condensation mechanism induced by exchange of atoms between the cluster and the surrounding gas seems to be different from our mechanism.